Proc. Natl. Acad. Sci. USA
Vol. 89, pp. 339–343, January 1992
Biophysics

Dynamics of single-motor molecules: The thermal ratchet model

(Brownian dynamics/myosin/model/motility)

NICOLÁS J. CÓRDOVA*, BARD ERMENTROUT†, AND GEORGE F. OSTER‡§

*Department of Applied Mathematics and Computer Science, Weizmann Institute of Science, Rehovot, Israel; †Department of Mathematics, University of Pittsburgh, Pittsburgh, PA 15260; and ‡Departments of Molecular and Cell Biology and Entomology, University of California, Berkeley, CA 94720

Communicated by Bruno H. Zimm, September 6, 1991 (received for review February 26, 1991)

ABSTRACT **We present a model for single-motor molecules—myosin, dynein, or kinesin—that is powered either by thermal fluctuations or by conformational change. In the thermally driven model, the cross-bridge fluctuates about its equilibrium position against an elastic restoring force. The attachment and detachment of the cross-bridge are determined by modeling the electrostatic attraction between the cross-bridge and the fiber binding sites, so that binding depends on the strain in the cross-bridge and its velocity with respect to the fiber. The model correctly predicts the empirical force–velocity characteristics for populations of motor molecules. For a single motor, the apparent cross-bridge step size per ATP hydrolysis depends nonlinearly on the load. When the elastic energy driving the cross-bridge is generated by a conformational change, the velocity and duty cycle are much larger than is observed experimentally for myosin.**

Until recently, it was only possible to study the mechanics of the motor molecules—myosin, dynein, and kinesin—by measuring the behavior of a large population working in concert. Recently, however, several laboratories have succeeded in studying the motions produced by one or a few motor molecules (1, 2). However, most models describe not single cross-bridges but large populations (3) and so cannot be used to interpret this new data on single and small numbers of cross-bridges. To understand their data we need a mechanical model for a single-motor molecule. There are many models that focus on the kinetic steps in the power cycle and address the mechanical aspects of the power stroke in thermodynamic terms of the free energies involved (4–7). Thus, they too are not suitable for investigating the mechanics of individual cross-bridges.

What powers the cross-bridge cycle, conformational change or thermal energy? There are two views on this question. The model proposed by Huxley (3) and its elaboration by Huxley and Simmons (10) have been the most influential in studying muscle mechanics. This model appears to attribute the source of energy to thermal fluctuations of the S1 cross-bridge of myosin, with ATP hydrolysis playing the role of making the random walk of the myosin cross-bridge unidirectional. That is, ATP hydrolysis allows the myosin cross-bridge to act as a "thermal ratchet" (11). Several authors have elaborated this idea (12–15), but none of their models directly addresses the mechanics of force transduction in a single cross-bridge as we shall do here.

The opposing model is that the power stroke arises from a conformational change in the S1 cross-bridge. In this model binding of ATP deforms the myosin cross-bridge; this elastic strain energy is stored in the "cocked" conformation until the release of hydrolysis products triggers it to spring back to its original unstrained shape. Thus, the power stroke is generated by converting the binding free energy of ATP to elastic strain energy, and then triggering its release. We will call this the "conformational change" model. Which model is correct? Of course, thermal fluctuations play a role in the conformational change model, for the strained cross-bridge must also randomly hunt for its binding site, and these thermally induced deformations also store elastic strain energy in the cross-bridge. So we must state the question more precisely: What proportion of the cross-bridge force arises from elastic energy created by binding ATP vs. elastic deformation energy arising solely from the Brownian fluctuations of the unstrained molecule? We address this question by constructing a model that can incorporate both sources of power so that the mechanical consequences of the two theories can be compared. Note that, for both the thermal ratchet and the conformational change mechanisms, the alternation of strong and weak binding states accompanying the nucleotide hydrolysis cycle is necessary for generating a directional power stroke (7). In the following discussion we will not always discriminate between actin–myosin, dynein–tubulin, and kinesin–tubulin systems because we feel that the basic physical mechanism is the same for all molecular motors.

Thermal Ratchet Model

Equations of Motion. We begin by describing a cross-bridge model, which is driven by thermal energy. We describe the motion of the ith unbound cross-bridge as follows. Let x_i be the displacement of the ith cross-bridge from its equilibrium position, $\bar{x}_i$. Then the motion of the cross-bridge can be described by a Langevin equation (17):

$$f\frac{dx_i}{dt} = -\kappa(x_i - \bar{x}_i) + A(t), \qquad [1]$$

where inertial effects have been neglected, since the Reynolds number is $<<1$ (18, 19). Here f = frictional drag coefficient. When we model the cross-bridge as a sphere, f is given by the Stokes formula, $f = 6\pi r\eta = 6\pi\,(6 \times 10^{-7}\ \text{cm})\,(10^{-2}\ \text{g/cm·sec}) \cong 1.13 \times 10^{-7}\ \text{g/sec}$. In Eq. 1 κ is an elastic modulus that, by assuming a maximum cross-bridge force of about $5\ pN = 5 \times 10^{-7}$ dyne, gives $\kappa \approx 0.5\ \text{g/sec}^2$ (12), and $A(t)$ is the random force modeling the thermal fluctuations produced by the fluid environment. $A(t)$ obeys Gaussian statistics with mean zero and correlation function $\langle A(t)A(t')\rangle = 2kTf\delta(t - t')$ (20).

For N cross-bridges operating in tandem, we choose their equilibrium spacing, a, such that adjacent cross-bridges do not compete for binding sites. The binding sites are located a distance b apart, and we choose $b \equiv 1$ as our unit of length. When a cross-bridge binds to a site on the fiber, the equation of motion switches to $dx/dt = dy/dt$, where dy/dt is the velocity of the fiber:

$$f_c\frac{dy}{dt} = -\kappa \sum_{j=\text{bound}}^{N} (x_j - \bar{x}_j) + A(t) + L, \qquad [2]$$

The publication costs of this article were defrayed in part by page charge payment. This article must therefore be hereby marked "*advertisement*" in accordance with 18 U.S.C. §1734 solely to indicate this fact.

§To whom reprint requests should be addressed.

where f_c is the drag on the cross-bridge–fiber complex: $f_c = N_b f + f_{actin} = N_b f + 2\pi\eta l/[\ln(l/r) - 0.5]$. N_b is the number of cross-bridges attached; l and r are the length and radius of the actin filament, respectively; and L is the external load on the fiber. Because the effect of thermal fluctuations on the fiber–cross-bridge complex is much smaller than in the cross-bridge alone, we can neglect the random term in Eq. **2** when the number of cross-bridges is large. Fig. 1*A* summarizes the thermally driven cross-bridge power cycle.

Attachment and Detachment of the Cross-Bridge. The experiments of Vale *et al.* (21) demonstrate that the interaction between a dynein cross-bridge and tubulin is electrostatic; therefore, we model the interaction between the cross-bridge and the fiber by an attractive electrostatic potential, $V(\delta, \xi)$, with a range of attraction about 1 Debye length, $\delta \approx 0.6$ nm at physiological electrolyte conditions. Here we define the strain in the ith cross-bridge as $\xi_i \equiv (x_i - \bar{x}_i)/h$, where $h = 12$ nm is the maximum stroke length. Hence, only when the cross-bridge comes within a distance δ of the fiber binding site can it be captured by the attractive well.

Probability of binding. We model the probability per unit time that the cross-bridge is captured by an actin binding site, P^a, as follows (more realistic models can easily be constructed):

$$P^a(v, \xi; \delta) = H(\delta - |x_i - y_j|)\,\frac{1}{1 + \beta|v|}\,\alpha(\xi_i). \qquad [3]$$

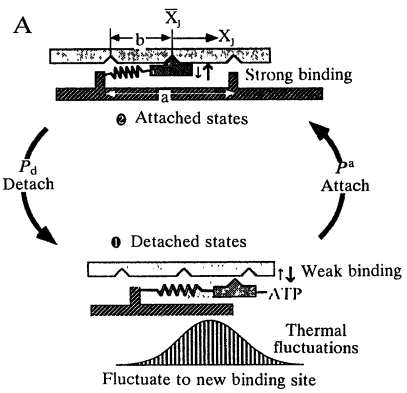

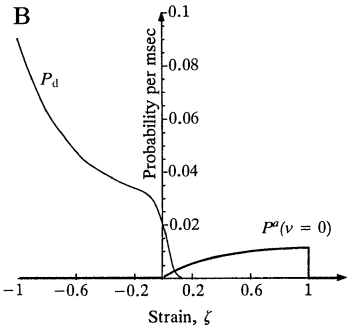

FIG. 1. (*A*) Thermal ratchet cross-bridge cycle. The model cycles through two kinetic states of attachment and detachment. The attached chemical states include: actin-myosin-ADP-P_i, actin-myosin-ADP, and actin-myosin. The detached states include: myosin-ATP and myosin-ADP-P_i. Binding of ATP weakens the attachment of the cross-bridge to the fiber, so that a small thermal fluctuation can detach the cross-bridge. The cross-bridge commences to fluctuate; eventually, a large enough fluctuation brings it within a Debye distance, δ, of the adjacent actin binding site. Hydrolysis of ATP relaxes the head enough to bind tightly to the site, and the cross-bridge pulls the fiber to the left towards its equilibrium position. During the stroke, hydrolysis products are released, restoring the system to its original attached configuration. (*B*) $P^a(\xi, v = 0) = \alpha(\xi)$ is the probability of attachment per unit time as a function of strain; $P_d(\xi)$ is the probability of dissociating from the well.

$H(\cdot)$ is the Heaviside step function ensuring that the capture probability is nonzero only when the cross-bridge is within a distance δ of the binding site whose coordinate is y_i. The second term is a geometrical factor giving the probability per unit time of the diffusing cross-bridge coming within δ of the binding site, which is moving past with velocity v. Although the results are quite insensitive to the exact shape of this function, we include this factor because our model is one-dimensional, while the actual motion of the head is three-dimensional. Therefore, the faster the fiber travels, the more likely it is that the head will not find the binding site before it moves out of range. The third term, $\alpha(\cdot)$, is an asymmetrical function that ensures that, as the cross-bridge moves to the right, its probability of capture increases monotonically. This binding asymmetry arises from the structural asymmetry of the cross-bridge (e.g., as the cross-bridge pivots to the right, its binding site is exposed) and the nucleotide hydrolysis cycle. However, we shall not model this in detail here but simply incorporate the effect phenomenologically by assuming that the probability of binding increases with strain as shown in Fig. 1*B*. In doing this, we are making the same assumption as the Huxley two-state model: that the concentration of ATP, ADP, and P_i are constant so that the binding and dissociation probabilities can be treated as functions of cross-bridge displacement (22).

Probability of detachment. After the completion of the power stroke, the cross-bridge must detach from the fiber to commence a new power cycle. The rate of dissociation is determined by the thermal energy required to knock the cross-bridge out of the fiber binding well. To extract work from the thermal environment, there must be an asymmetry in the binding potential, V, so that the cross-bridge is more likely to dissociate to the left of its equilibrium position. This asymmetry in dissociation is produced by the nucleotide hydrolysis cycle, which we are not explicitly modeling here. However, we can model the effect of nucleotide binding by assuming that the potential well has a deep and a shallow state, which we denote by **S** (strong binding) and **w** (weak binding) (7). The transition from **S** to **w**, which occurs upon binding of nucleotide, depends on the displacement of the cross-bridge to the left of its equilibrium position. When the cross-bridge is bound in the weak state, it may not detach instantly: it must wait for a large enough thermal fluctuation to dislodge it from the electrostatic well. We can include the physics of this event as follows.

The depth of the well is $V(\xi)$, but because the cross-bridge is displaced from its equilibrium position, the well attraction is opposed by the spring elastic energy. Thus, the dissociation probability per unit time from the binding state is given by the Boltzmann probability (20):

$$P_d(\xi) \propto e^{-\left(\frac{V(\xi) - \frac{\kappa}{2}(h\xi)^2}{kT}\right)}. \qquad [4]$$

This attachment/detachment model contains some of the physics of the association and dissociation process; however, the essential ingredient of dissociation asymmetry is modeled phenomenologically as shown in Fig. 1*B*. Various shapes for the probabilities of binding/unbinding have been used to fit experimental data on muscle contraction, and it turns out that the detailed shape of the probability functions is not critical (5, 8, 15). Note that because we have neglected reverse reactions, the probabilities of binding and detachment do not exactly obey thermodynamic detailed balance; addition of a small reversible ATP cycle does not significantly affect the model's predictions (5, 8, 22).

The model for a single cross-bridge consists of Eqs. **1–4**. Note that while Eqs. **1** and **2** are linear, the model is nonlinear

because of the probabilistic switch between free and bound states governed by Eqs. **3** and **4**.

Dynamics of the Thermal Ratchet Model

In this section we show how the thermal ratchet model can reproduce many of the empirical observations on motor molecules. We used a fourth-order Runge–Kutta algorithm to integrate the equations of motion. The parameters used in the simulations to study actin–myosin systems are listed in Table 1.

Steady-State Behavior of Large Populations of Cross-Bridges. If we plot the fiber position vs. time for various loads, a linear least-squares fit to the time series yields the average fiber velocity (see Fig. 3). A series of such calculations under various loads enables one to compute the steady-state load–velocity response for a single cross-bridge and for multiple cross-bridges. For a single cross-bridge, the velocity decreases nonlinearly with load as shown in Fig. 2. When many cross-bridges are operating simultaneously, the velocity dependence of the binding and the probabilistic nature of detachment depress the graph still more below linearity. Fig. 2 shows that 350 cross-bridges acting in parallel fit well the hyperbolic shape of Hill's empirical equation (24): $L^* = (1 - v^*/(1 + v^*/a)$, where $v^* = v/v_{max}$, $L^* = L/L_{max}$. L_{max} is the isometric load, and v_{max} is the no-load velocity; for most skeletal muscles: $0.15 \leq a \leq 0.25$. Moreover, the model exhibits a discontinuity in the slope of the force–velocity curve at zero velocity, in agreement with Katz (25).

By tethering a fiber to a glass microneedle and observing the displacement, Chaen *et al.* (23) were able to study a population of myosin motors under "auxotonic" conditions; that is, a displacement-dependent load. The force velocity curve they obtained was concave, in contrast to the convex shape of the Hill plot. We simulated this situation by having the motor population push against a linear spring. The results are shown in Fig. 2, which reproduces the concave feature of these experiments quite well.

Dynamics of Small Populations of Cross-Bridges. *In vitro* assays now make it possible to study the motion of fibers driven by but a few cross-bridges, and so it is informative to look at the dynamics of fiber motion under these circumstances when their statistical behavior becomes important.

A cross-bridge cycles between attached and detached states, but the amount of time it spends in each state is a random variable that depends on the load. Fig. 3*A* shows a "microscopic" view of a fiber's motion when it is being driven by a small number of cross-bridges.

One of the fundamental issues our model attempts to address is: what is the physical mechanism by which chemical energy is transduced into mechanical motion? In this connection, an important disagreement has arisen in the literature over the step size of the myosin cross-bridge. That is, how far does a cross-bridge travel along the fiber in one

Table 1. Parameter values used in simulations

Parameter	Description	Value
f	Myosin friction coefficient	1.13×10^{-7} g/sec
κ	Myosin elastic modulus	0.5 g/sec^2
δ	Debye length	0.6 nm
β	Steric velocity parameter	4×10^3 sec/cm
S	Strong binding potential depth	15 kT
w	Weak binding potential depth	1 kT
a	Equilibrium spacing of cross-bridges	33 nm
b	Spacing of actin binding sites	10 nm
h	Myosin stroke length	12 nm
l	Length of actin filament	1–3 μm
r	Radius of actin filament	5.5 nm
Δt	Integration time step	10^{-7}–10^{-6} sec
N	No. of active cross-bridges	1–350

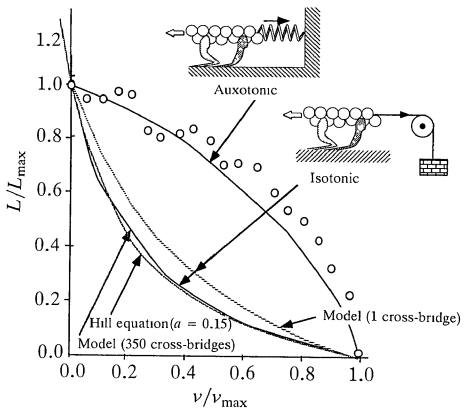

FIG. 2. Reduced tension, or load, L/L_{max}, as a function of the reduced velocity, v/v_{max} for 1 and 350 cross-bridges. Here L_{max} is the isometric load (i.e., the load just sufficient to arrest the motion, $v = 0$), and v_{max} is the maximum velocity (i.e., at zero load). The model fits the Hill equation with $a = 0.15$. Also shown is the tension–velocity curve for a population of 350 cross-bridges when the motors are working against a linear spring. The model curve is close to the measurements of Chaen *et al.* (23) at small loads.

ATP hydrolysis cycle? This is a crucial point, for if the step size is larger than the span of the cross-bridge, then the transduction mechanism must be such that the cross-bridge can "fractionate" the free energy of hydrolysis so as to make many strokes per hydrolysis. This possibility has given rise to models that contravene the classical rotating cross-bridge picture (12, 14).

Several laboratories have estimated the apparent myosin step size and come up with quite different results, ranging from 5 to 120 nm (1, 18, 26–29). The difficulty in these experiments is that one cannot measure the power stroke directly, since it is not possible to observe the motion of a cross-bridge. Instead one must infer the displacement from the velocity of the fiber, v_f, and the ATP hydrolysis rate, $R = d[ATP]/dt$. To do this, one must know the number of cross-bridges operating and make some assumption about the number of ATP cycles per power stroke. For example, if there were but one hydrolysis per power stroke, then the mean cycle time for a cross-bridge would be $\bar{T}_c \propto 1/R$. Can one estimate the average step size, $\bar{\Delta}_{est}$, from $\bar{T}_c$ and the average fiber velocity, $\bar{v}_f$? One estimate is obtained by dividing the average fiber velocity, $\bar{v}_f$, by the hydrolysis rate: $\bar{\Delta}(T_c, N) = \bar{v}_f(N) \cdot T_c = \bar{v}_f(N)/R$. However, at zero load, the fiber spends <10% of its time in the power stroke; only at about 0.4 v_{max} does the head spend an appreciable time in contact with the fiber. Therefore, one might estimate step size as: $\bar{\Delta}(t_s, N) = \bar{v}_f(N) \cdot \bar{t}_s$, where the average stroke time, $\bar{t}_s$, is the time the cross-bridge is bound to the fiber (1, 26). Both estimates depend on knowing the number of cross-bridges driving the fiber. The relationship between the "true" mean step size, $\bar{\Delta}$, and the estimates based on $\bar{T}_c$ and $\bar{t}_s$ are shown in Fig. 3*B*.

Step-size measurements in large populations can be misleading. For example, for $N > 20$, $\bar{v}_f$ does not depend on N (Fig. 3*A Inset*); therefore, one might think it reasonable to correct for the stroke time by counting only cross-bridges that are actually attached by multiplying by the average fraction of attached cross-bridges, ϕ_a: $\Delta' = \bar{\phi} \cdot \bar{T}_c \cdot \bar{v}_f$. Computed this way, the cross-bridges appear to be making steps far longer than the dimensions of the molecule, as high as 120 nm! Only when the fiber is loaded so that it moves much slower than its maximum velocity is Δ' close to the actual step size. This points to the necessity of measuring velocities at high loads and with few cross-bridges to accurately estimate the step size from fiber velocity and ATP rate measurements.

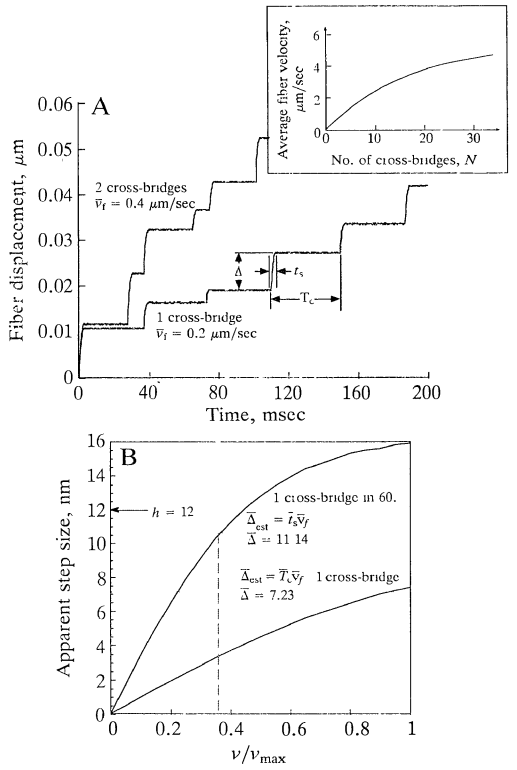

FIG. 3. (*A*) Motion of a fiber driven by 1 and 2 cross-bridges. Since each cross-bridge is a linear elastic element and binding and detachment are random processes, the power strokes are exponentials with random slopes and asymptotes; between power strokes, the fiber fluctuates about its mean position. The stroke time, t_s, cycle time, T_c, and step size, Δ, are also random variables. At zero load, the average stroke time, $\bar{t}_s << \bar{T}_c$, so that each cross-bridge spends most of its time detached and hunting for a binding site, while the fiber spends most of its time stationary. For one cross-bridge, $\bar{t}_s$ = 3.2 ± 0.062 msec, $\bar{T}_c$ = 37.3 ± 0.8 msec (± refers to the standard deviation). The average "duty ratio" ($\overline{t_s/T_c}$) drops from 0.08 for 1 cross-bridge to 0.04 for 20 cross-bridges as their duty cycles begin to overlap; this means that as the number of cross-bridges increases, each cross-bridge spends less time working. The mean stepsize for 1 cross-bridge is $\bar{\Delta}$ = 7.23 ± 2.24 nm, which is less than the actual step size of h = 12 nm. For 1 cross-bridge in a population of 80, the mean stepsize rises to $\bar{\Delta}$ = 11.14 ± 5.56 nm. The average fiber velocity, $\bar{v}_f$, is computed from a least squares curve through the trajectory. For one cross-bridge, $\bar{v}_f$ (N) is fit well by $\bar{v}_f = 5.4(1 - e^{-0.06N})$ [*Inset*]; this is almost the same as the function employed by Uyeda *et al.* (26): $v = v_{max}[1 - [1 - (t_s/T_c)]^N]$, where they estimated a duty ratio of 0.05. (*B*) The apparent step size depends on how it is estimated. The curves show how the estimated step sizes vary as a function of load for 1 cross-bridge and for one in a population of 60 cross-bridges. For a single cross-bridge, at zero load the estimated step size is quite close to the actual mean step size; for a population of cross-bridges, however, the estimated and actual step sizes are only the same at about 0.35 v_{max}.

Our simulation studies are consistent with the experiments of Uyeda *et al.* (1, 26) and support the idea that each stroke requires a nucleotide hydrolysis. There is no necessity for fractionating the free energy of ATP hydrolysis to fit the model to their data. It is possible that the large step sizes estimated by Yanagida and coworkers (28, 29) are partially due to differences in fiber loading and/or their estimations of the stroke times.

Conformational Change Model

A fundamental question is whether the cross-bridge is powered by thermal fluctuations or by a conformational change. That is, does the ATP hydrolysis cycle simply rectify thermal motion or is the binding energy of the nucleotide to the head transduced into elastic energy of deformation? Our calculations show that the thermal ratchet model can reproduce much of the data on cross-bridge statistics. However, this does not prove that the sole source of power is thermal fluctuations, for it is possible that a conformational change could fit the data as well. To investigate this possibility we have added conformational change to the model so that we can compare the performance of the two mechanisms.

According to the conformational change model, binding of nucleotide to the head has two concurrent effects. First, it weakens the binding of the head to the fiber, allowing it to be released from the rigor complex (7), and second, it deforms the head to a new equilibrium position. Thus, the free energy of nucleotide binding is transduced into elastic strain energy in the head. When the head binds to the fiber, some of this strain energy could be released to drive the fiber. In terms of our model, this means that, upon detachment from the fiber, the equilibrium position of the head shifts to the right, as shown in Fig. 4 *Inset*. Since the two-state model has only one bound state, at the moment of binding, the equilibrium position reverts to its original value. Therefore, if the head finds its binding site at a displacement x_{bind}, then an amount of elastic energy $E_{elas} = \kappa x_{bind}^2$ (shown shaded in Fig. 4 *Inset*) can be used to drive the fiber; of this, only $\kappa(x_{bind} - x_o)^2/2$ has been generated by Brownian motion of the head.

The effect of conformational change is to dramatically increase the fiber velocity far beyond the observed values. Moreover, the duty cycle, t_s/T_c, increases to nearly 30%, which is much higher than is measured experimentally (26). The reason for this is that the conformational change x_o brings the head to the vicinity of its binding site much more quickly than if it had to wait for a sufficiently large thermal fluctuation. To bring the velocity and attachment time back to

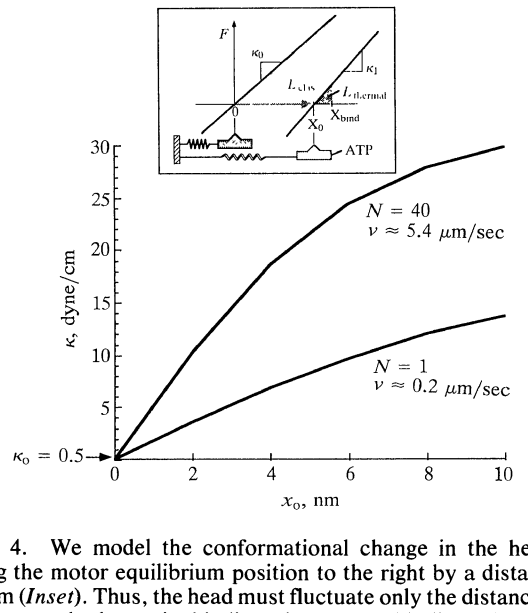

FIG. 4. We model the conformational change in the head by shifting the motor equilibrium position to the right by a distance x_o = 10 nm (*Inset*). Thus, the head must fluctuate only the distance $x_{bind} - x_o$ to reach the actin binding site. Upon binding, the elastic modulus and the rest displacement revert to their original values. Thus, an amount of elastic energy $E_{elas} = \kappa x_{bind}^2$ is available to drive the fiber, but only $E_{thermal} = \kappa(x_{bind} - x_o)^2/2$ had been generated by thermal fluctuations of the cross-bridge. To reproduce experimental fiber velocities, the elastic modulus of the head must be increased as the size of the conformational change increases. The curves show how much κ must increase for a given conformational change so as to match the observed velocities for one cross-bridge ($v \approx 0.2$ μm/sec), and for 40 cross-bridges ($v \approx 5.4$ μm/sec). For a conformational change equivalent to the entire power stroke, x_o = 12 nm, the elastic constant must be increased by a factor of 60 to slow a fiber driven by 40 cross-bridges to the observed velocity of about 5.4 μm/sec. For a single cross-bridge, a factor of nearly 24 is required.

observed values, the elastic constant of the head must be increased considerably. In Fig. 4 we have plotted the elastic constant, κ, and conformational change, x_o, required to reproduce normal fiber velocities for one cross-bridge and for 40 cross-bridges. If the rate of nucleotide hydrolysis were much slower than the time the head takes to detach and rebind, then hydrolysis would be the rate-limiting step; only when the mechanics is rate-limiting can the two-state model detect the effect of conformational change by observing the fiber motion. Thus, the two-state model supports the notion that myosin cross-bridges are powered largely by thermal motion and that shape changes induced by the binding of nucleotide do not contribute substantially to force production. However, a full investigation of the effects of conformational change requires explicit modeling of the hydrolysis cycle.

Discussion

To investigate how thermal energy is transduced into unidirectional motion, we have used computer simulation to follow the motion of a single-motor molecule. In the thermal ratchet model, the nucleotide hydrolysis does not provide the energy for the power stroke—that comes from thermal fluctuations. Instead, nucleotide hydrolysis plays the role of a "Maxwell's Demon": to rectify the random fluctuations of the cross-bridge to produce a net force in one direction. We mimicked the nucleotide hydrolysis cycle by an electrostatic attachment model with asymmetric probability functions for attachment and detachment. Thermal energy controls the model's behavior in three different ways: (*i*) the force developed by a cross-bridge is provided by the Brownian fluctuations that deform the elastic element in the cross-bridge, (*ii*) thermal vibrations of the cross-bridge allow it to hunt for an actin binding site, and (*iii*) during or after completion of the power stroke, thermal fluctuations dislodge the myosin cross-bridge from the potential well holding it to the actin fiber.

Although our model is of a single motor molecule, most quantitative mechanical data have been obtained from myosin populations, mostly in muscle fibers. Therefore, we have compared the model's performance with these published measurements. We find that it fits quite well the concave force–velocity curve (Hill plot) and the convex "auxotonic" response measurements of Chaen *et al.* (23). The model is also consistent with the force–velocity curve obtained from quick release experiments with frog muscles. For example, the negative slope of the force–velocity curve for slow stretching was predicted to be 4.5 times greater than the negative slope for slow shortening (25). We also found that, because the Debye length affects binding and dissociation differently, the model predicts that the velocity of motor molecules is dependent on the ionic strength, in accord with *in vitro* experiments (12).

There is much disagreement about the step size of motor molecules, and so we have addressed this issue by computing the apparent step size as determined by macroscopic measurements on fiber velocity and nucleotide hydrolysis rates. We find that the "apparent" step size is a nonlinear, monotonically increasing function of velocity. Depending on the method used to estimate the stroke time, it could appear to be as large as 120 nm, even though the actual step size of the model is 12 nm. This load dependence could be a partial explanation for the variety of different results reported by different laboratories. The possibility of a step size much larger than the actual stroke length also has been addressed by Leibler and Huse (16) using a different stochastic model, and they also conclude that apparent step sizes can far exceed the actual step size.

Finally, we have computed that, if myosin cross-bridges undergo a conformational change, they will drive an actin fiber faster and with much higher duty ratios (stroke time per cycle time) than is observed—providing all other model parameters remain the same. This suggests that myosin may be powered almost exclusively by thermal energy, with the spatial asymmetry in the binding/unbinding controlled by the ATP dynamics. Other motor molecules such as kinesin, which remain attached to microtubules for a large fraction of their cycle, may employ conformational change to partially power their working stroke.

We modeled the detachment asymmetry here by assuming a strain-dependent electrostatic binding potential as a surrogate for including the dynamics of nucleotide binding, similar to Huxley's two-state model. To address the partition of force generation into conformational and thermal contributions properly, we must explicitly add several attached states—in effect, modeling the nucleotide hydrolysis cycle.

We thank Roger Cooke, Paul Janmey, Stanislas Leibler, Dan Lerner, Gary Odell, Ed Pate, Tim Ryan, Manfred Schliwa, Robert Simmons, Michael Weliky, and Bruno Zimm for valuable conversations during the course of this work, with special thanks to Jim Spudich and Ron Vale for insightful conversations on experimental matters and for sharing unpublished work with us. This work was initiated at the Neurosciences Institute of the Neurosciences Research Program in New York, and we thank the Institute for its gracious hospitality and intellectual environment. G.F.O. was supported by National Science Foundation Grant MCS-8110557 and a MacArthur Foundation Fellowship. N.J.C. was partially supported by U.S.–Israel Binational Science Foundation Grant 3777. B.E. was supported by National Science Foundation Grant DMS9002028.

1. Uyeda, T., Warrick, H., Kron, S. & Spudich, J. (1991) *Nature (London)* **352,** 307–311.
2. Howard, J., Hudspeth, A. J. & Vale, R. D. (1989) *Nature (London)* **342,** 154–158.
3. Huxley, A. F. (1957) *Prog. Biophys. Biophys. Chem.* **7,** 255–318.
4. Pate, E. & Cooke, R. (1989) *J. Muscle Res. Cell Motil.* **10,** 181–196.
5. Hill, T., Eisenberg, E., Chen, Y. & Podolsky, R. (1975) *Biophys. J.* **15,** 335–372.
6. Eisenberg, E., Hill, T. & Chen, Y. (1980) *Biophys. J.* **29,** 195–227.
7. Eisenberg, E. & Hill, T. (1985) *Science* **227,** 999–1006.
8. Brokaw, C. J. (1976) *Biophys. J.* **16,** 1013–1027.
9. Chen, Y. & Hill, T. L. (1988) *Proc. Natl. Acad. Sci. USA* **85,** 431–435.
10. Huxley, A. & Simmons, R. (1971) *Nature (London)* **233,** 533–538.
11. Feynman, R., Leighton, R. & Sands, M. (1963) *The Feynman Lectures on Physics*, (Addison-Wesley, Reading, MA).
12. Vale, R. D. & Oosawa, F. (1990) *Adv. Biophys.* **26,** 97–134.
13. Meister, M., Caplan, S. R. & Berg, H. C. (1989) *Biophys. J.* **55,** 905–914.
14. Mitsui, T. & Ohshima, H. (1988) *J. Muscle Res. Cell Motil.* **9,** 248–260.
15. Smith, D. A. & Sicilia, S. (1987) *J. Theor. Biol.* **127,** 1–30.
16. Leibler, S. & Huse, D. (1991) *C.R. Acad. Sci. Paris* **313,** 27–35.
17. Riskin, H. (1989) *The Fokker-Planck Equation*, (Springer, New York).
18. Ishijima, A., Doi, T., Sakurada, K. & Yanagida, T. (1991) *Nature (London)* **352,** 301–306.
19. Yanagida, T., Arata, T. & Oosawa, F. (1985) *Nature (London)* **316,** 366–369.
20. Chandrasekhar, S. (1943) *Rev. Mod. Phys.* **15,** 1–89.
21. Vale, R., Soll, D. & Gibbons, I. (1989) *Cell* **59,** 915–925.
22. Woledge, R., Curtin, N. & Homsher, E. (1985) *Energetic Aspects of Muscle Contraction* (Academic, New York).
23. Chaen, S., Oiwa, K., Shimmen, T., Iwamoto, H. & Sugi, H. (1989) *Proc. Natl. Acad. Sci. USA* **86,** 1510–1514.
24. McMahon, T. (1984) *Muscles, Reflexes, and Locomotion*, (Princeton Univ. Press, Princeton, NJ).
25. Katz, B. (1939) *J. Physiol. (London)* **96,** 45–64.
26. Uyeda, T., Kron, S. & Spudich, J. (1990) *J. Mol. Biol.* **214,** 699–710.
27. Harada, Y. & Yanagida, T. (1989) *Prog. Clin. Biol. Res.* **315,** 27–36.
28. Yanagida, T. & Harada, Y. (1988) *Adv. Exp. Med. Biol.* **226,** 277–287.
29. Harada, Y., Sakurada, K., Aoki, T., Thomas, D. D. & Yanagida, T. (1990) *J. Mol. Biol.* **216,** 49–68.